Optica Applicata, Vol. XII, No. 2, 1982

Spectral responses of the *n*-PbTe/*p*-$Pb_{1-x}Sn_xTe$ heterojunctions

WALDEMAR LARKOWSKI, ANTONI ROGALSKI
Institute of Technical Physics, Military Academy of Technology, 00-908 Warsaw, Poland.

The influences of the Burstein-Moss effect on the spectral dependence of the absorption coefficient for $Pb_{1-x}Sn_xTe$ and on the spectral characteristics of the *n*-PbTe/*p*-$Pb_{1-x}Sn_xTe$ heterojunctions have been analysed. It has been pointed out that for carrier concentration in $Pb_{1-x}Sn_xTe$ above 10^{25} m^{-3} the spectral cutoff of the heterojunction is determined by the PbTe material used. It has been also attempted to fit the characteristics calculated theoretically for this kind of heterojunctions with those measured experimentally.

1. Introduction

The narrow-gap semiconductors $Pb_{1-x}Sn_xTe$ are widely used in the infrared technique. This is the basic material used in production of photodiodes of various structures, among them homojunctions, heterojunctions as well as Schottky junctions. Heterojunctions *n*-PbTe/*p*-$Pb_{1-x}Sn_xTe$ are produced mainly by liquid phase epitaxy by depositing the Pb_{1-x} Sn_xTe semiconductor layer of narrower energy gap onto a single crystal substrate of PbTe [1–3] or to deposit successively, first the $Pb_{1-x}Sn_xTe$ layers and then the PbTe [4–8]. Some attempts have been also made to produce the heterojunctions by the hot-wall epitaxy technique [9–13]. In all the cases the heterojunctions are illuminated from the PbTe side, i.e., from the side of semiconductor of wider energy gap. The advantage offered by heterojunction structure is that the radiation of the wavelength outside the PbTe absorption edge is absorbed in $Pb_{1-x}Sn_xTe$ far from photodiode surface. There are no losses caused by surface recombination in the case of thick PbTe region. The application of the semiconductor of greater energy gap on one side of the junction diminishes the value of the saturation current for the non-illuminated photodiode and by the same means increases the differential resistance of the diode for polarization equal to zero.

Various spectral responses of photodiodes have been obtained, the spectral cutoff λ_c of which was not always determined by the $Pb_{1-x}Sn_xTe$ material. In the works [9, 10, 12] the spectral responses have been measured, long wavelength edge of which was determined by PbTe. The λ_c shift may be influenced by:

i) The concentration level in $Pb_{1-x}Sn_xTe$ as well as the associated Burstein-Moss shift and the carrier life-time.

ii) The diffusion process in the PbTe-$Pb_{1-x}Sn_xTe$ interface occurring during the heterostructure production — the influence of this process being essential when the heterostructure is produced at high temperature [8].

In order to interpretate in a convincing way the different types of measured spectral response for n-PbTe/p-$Pb_{1-x}Sn_xTe$ the calculations of these characteristics made in the present work for different carrier concentrations in $Pb_{1-x}Sn_xTe$ and different depths of junction were performed by neglecting the influence of the diffusion on PbTe-$Pb_{1-x}Sn_xTe$ interface (this topic is discussed in [8]). Also, some attempts were made to fit the theoretically calculated responses to those measured experimentally. Since the knowledge of the dependence of the absorption coefficient for PbTe and $Pb_{1-x}Sn_xTe$ upon the wavelength and the carrier concentration is necessary to perform the calculations also this problem was dealt with.

2. Absorption coefficient

Interband absorption in lead and tin chalcogenides is a more complex phenomenon than in semiconductor of parabolic bands. This is caused by:

i) anisotropic and multi-valley structure of both conduction and valence bands,

ii) non-parabolic energy dispersion.

iii) dependence of matrix elements on momentum operator k.

In papers [14, 15] the interband absorption was discussed in the lead and tin chalcogenides based on six-band Dimmock model and two band Kane model. A good agreement has been achieved between theoretical calculation results and those obtained in experimental measurements of the spectral dependence of the absorption coefficient for $Pb_{1-x}Sn_xTe$ at the vicinity of the absorption edge [15]. However, for photon energy above 1.5 E_g the experimental coefficients of absorption were higher than those calculated theoretically, while the discrepancies were greater for Dimmock model. The dependence of absorption coefficient upon the composition x and the temperature at the absorption edge vicinity is better described by the Kane model [15].

For lead and tin chalcogenides the absorption coefficient, according to Kane model, has the form [14]

$$\alpha_{(z)} = \frac{E_g}{n_r} K_* (z-1)^{1/2} f(z) (f_v - f_c), \tag{1}$$

where E_g – energy gap, n_r – refraction coefficient, $f(z) = (1+z)^{1/2}(1+2z)^2/(3\sqrt{2}z^2)$, $z = h\nu/E_g$, h – Planck constant, ν – radiation frequency, f_v and f_c – Fermi-Dirac functions for holes and electrons, respectively.

The last term in the expression (1) takes into account band-filling. From the analysis of the absorption band for $Pb_{1-x}Sn_xTe$ of the composition $0 \leqslant x \leqslant 0{,}21$ within the temperature range $90 \leqslant T \leqslant 300$ K given in [14] the value of $K = (6.5 \pm 1.5) \cdot 10^5\ \mathrm{eV}^{-1}\ \mathrm{cm}^{-1}$ is reported.

In the case of Boltzmann statistics valid for the nondegenerated semiconductors when the conduction and valence bands are empty, the last term in the

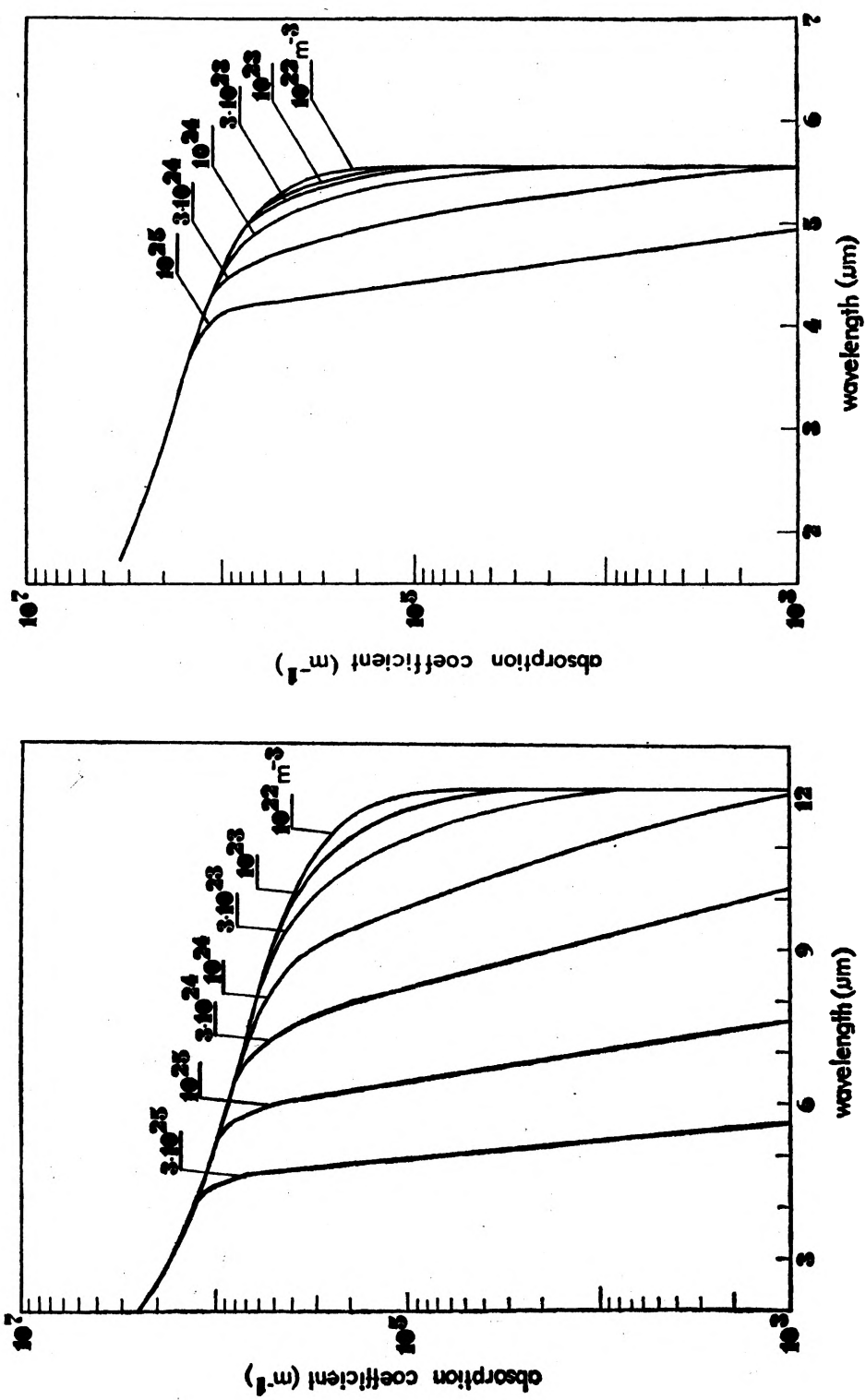

Fig. 1. Influence of the Burstein-Moss effect on the absorption coefficient upon the wavelength at 77 K for: a. PbTe, b. $Pb_{0.78}Sn_{0.22}Te$

expression (1) is equal to unity. As the band is being populated – which affects essentially the spectral dependence of the absorption coefficient – $(f_v - f_c)$ diminishes, which is the so-called Burstein-Moss effect. Fig. 1 shows the influence of the carrier concentration on the absorption coefficient dependence upon the wavelength for PbTe and $Pb_{0.78}Sb_{0.22}Te$ at the temperature of 77 K. The calculations have been based on the expression (1), taking $K_* = 6.5 \cdot 10^5\ eV^{-1}cm^{-1}$ [14] and $n_r = 6.5$ and 7.2 for PbTe [16], and $Pb_{1-x}Sn_xTe$ [17], respectively. The position of Fermi level, necessary to determine $(f_v - f_c)$, has been calculated in the way described in Appendix. From Fig. 1 it may be noted that, as the concentration increases, the absorption band suffers from the spreading being simultaneously shifted toward the shorter wavelength. Besides, for the given carrier concentration the Burstein-Moss shift is of greater influence for semiconductors of less energy gap width (of less effective masses) as it is the case for $Pb_{0.78}Sn_{0.22}Te$.

3. Spectral responses

In Figure 2 the band structure for a typical heterojunction is presented. The total quantum efficiency is the result of contribution from four regions: two neutral regions of opposite types of conduction and two regions of space charge of widths w_1 and w_2, respectively. In accordance with this we have

$$\eta = \eta_n + \eta_{DR}^n + \eta_{DR}^p + \eta_p, \tag{2}$$

where η_{DR}^n and η_{DR}^p denote the quantum efficiencies of the space charge regions in the n-type and p-type semiconductors, respectively. The particular components of the quantum efficiency have the forms [18]:

$$\eta_n = \frac{\alpha_1 L_h}{\alpha_1^2 L_h^2 - 1}\left\{\frac{\alpha_1 L_h + \gamma_1 - e^{-\alpha_1 x_h}[\gamma_1 ch(x_n/L_h) + sh(x_n/L_h)]}{\gamma_1 sh(x_n/L_h) + ch(x_n/L_h)} - \alpha_1 L_h e^{-\alpha_1 x_n}\right\}, \tag{3}$$

$$\eta_p = \frac{\alpha_2 L_e}{\alpha_2^2 L_e^2 - 1} e^{-\alpha_1 t} e^{-\alpha_2 w_2}, \tag{4}$$

$$\times\left\{\alpha_2 L_e - \frac{\gamma_2\left[ch[(d-w_2)/L_e] - e^{-\alpha_2(d-w_2)}\right] + sh[(d-w_2)/L_e] + \alpha_2 L_e e^{-\alpha_2(d-w_2)}}{\gamma_2 sh[(d-w_2)/L_e] + ch(d-w_2)/L_e}\right\},$$

$$\eta_{DR}^n = e^{-\alpha_1 x_n}(1 - e^{-\alpha_1 w_1}), \tag{5}$$

$$\eta_{DR}^p = e^{-\alpha_1 t}(1 - e^{-\alpha_2 w_2}), \tag{6}$$

where α_1 and α_2 – absorption coefficients in n-type and p-type regions, respectively, $\gamma_1 = s_1 L_h/D_h$, $\gamma_2 = s_2 L_e/D_e$, L_e and L_h – diffusion length for electrons and holes, respectively, D_e and D_h – coefficients of diffusion for electrons and holes, respectively, s_1 and s_2 – surface recombination velocities for illuminated and back photodiode surfaces, respectively.

The above formulae do not take account of the losses caused by the reflection of the radiation on the illuminated surface of the heterojunction. In order to encounter also these losses the expressions should be multiplied by $(1-r)$. Additionally, the expressions (4) and (6), have been derived by neglect-

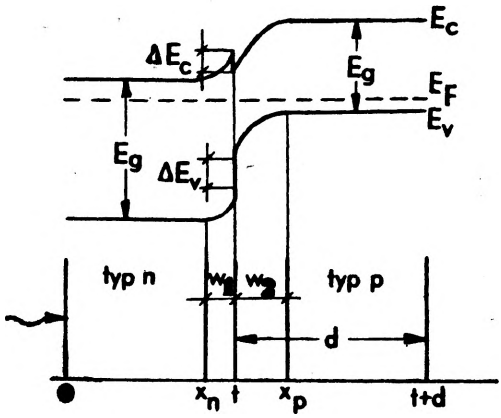

Fig. 2. Band structure of the heterojunction

ing the radiation reflection on the interface surface $x = t$. This reflection is conditioned by the refractive index difference in the n- and p-type regions. They can be taken into account by replacing the term $\exp(-\alpha_1 t)\exp(-\alpha_2 w_2)$ by a more complex transmission factor given by MILNES and FEUCHT [19]. Because of the similar values of the refraction coefficient for PbTe and $Pb_{0.8}Sn_{0.2}Te$ the reflection is close to zero and may be neglected.

The charge space widths w_1 and w_2 are determined by the relative doping levels and dielectric constants for semiconductors on both sides of junctions [18]:

$$w_1 = \left[\frac{2\varepsilon_1}{qN_1}\frac{\varepsilon_2 N_2}{\varepsilon_1 N_1+\varepsilon_2 N_2}V_{bi}\right]^{1/2},$$

$$w_2 = \left[\frac{2\varepsilon_2}{qN_2}\frac{\varepsilon_1 N_1}{\varepsilon_1 N_1+\varepsilon_2 N_2}V_{bi}\right]^{1/2},$$

where $V_{bi} = 1/q(E_{Fp}-E_{Fn})$ is the diffusion potential (E_{Fn} and E_{Fp} denote the energy at the Fermi level of isolated semiconductors creating the respective region of n- and p-types of the heterojunction).

The relations (3) and (4) are derived under assumptions that the concentrations of excess minority carriers close to the edge of the space charge region are reduced to zero by the electric field in the depletion region. Such an assumption is justified under the condition that the discontinuity of energy in the conduction (valency) band $\Delta E_c(\Delta E_v)$ is small ($< kT/q$) in n/p (p/n) heterojunction [18]. In the opposite case the minority carriers from the region of less energy gap may be impeded during the current flow through the junction, which results consequently in diminishing the photocurrent (for example, an electron moving

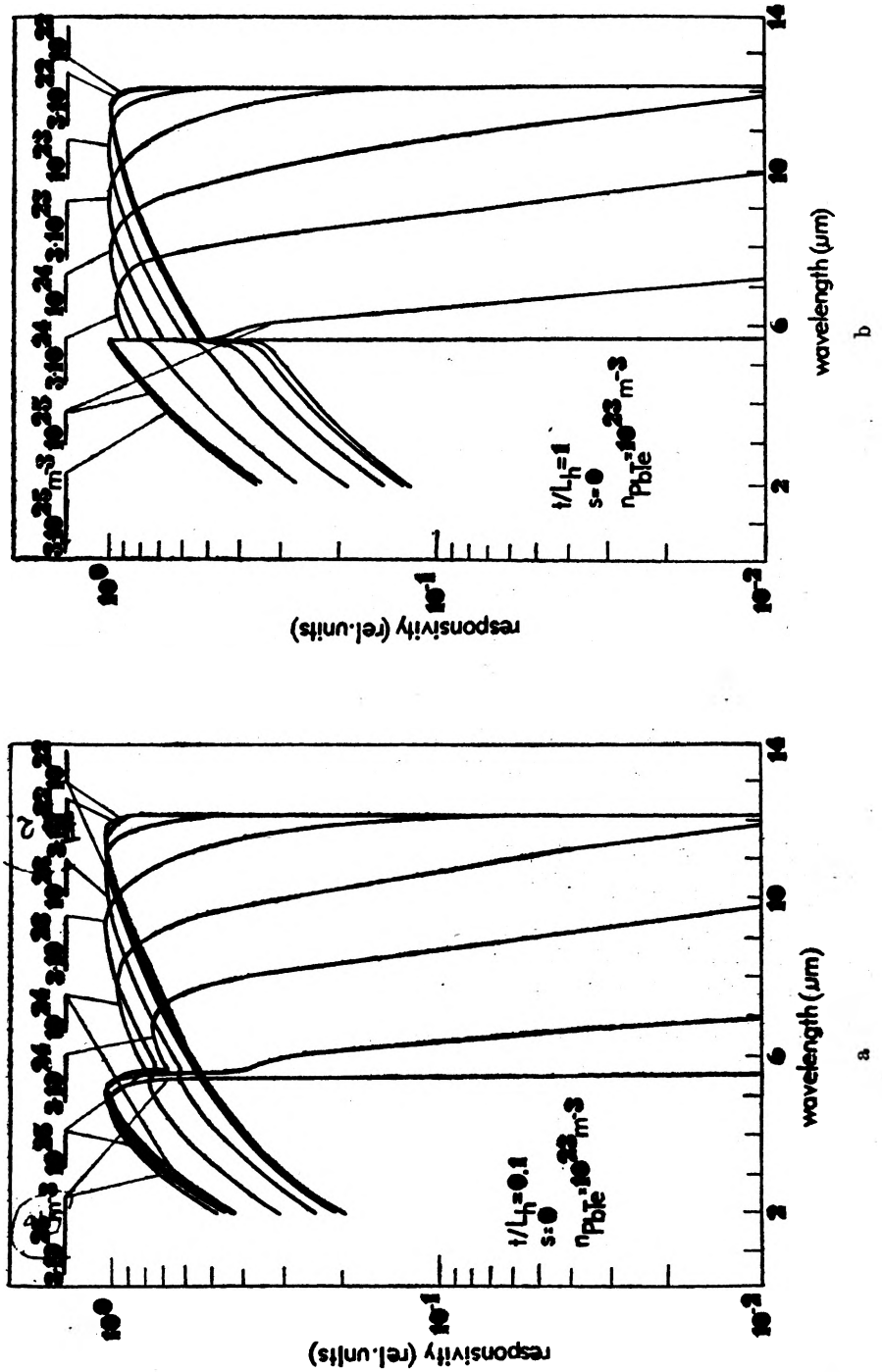
responsivity (rel.units)
wavelength (μm)
t/L_h=0.1
s=0
n_PbTe=10^23 m^-3
a
responsivity (rel.units)
wavelength (μm)
t/L_h=1
s=0
n_PbTe=10^23 m^-3
b

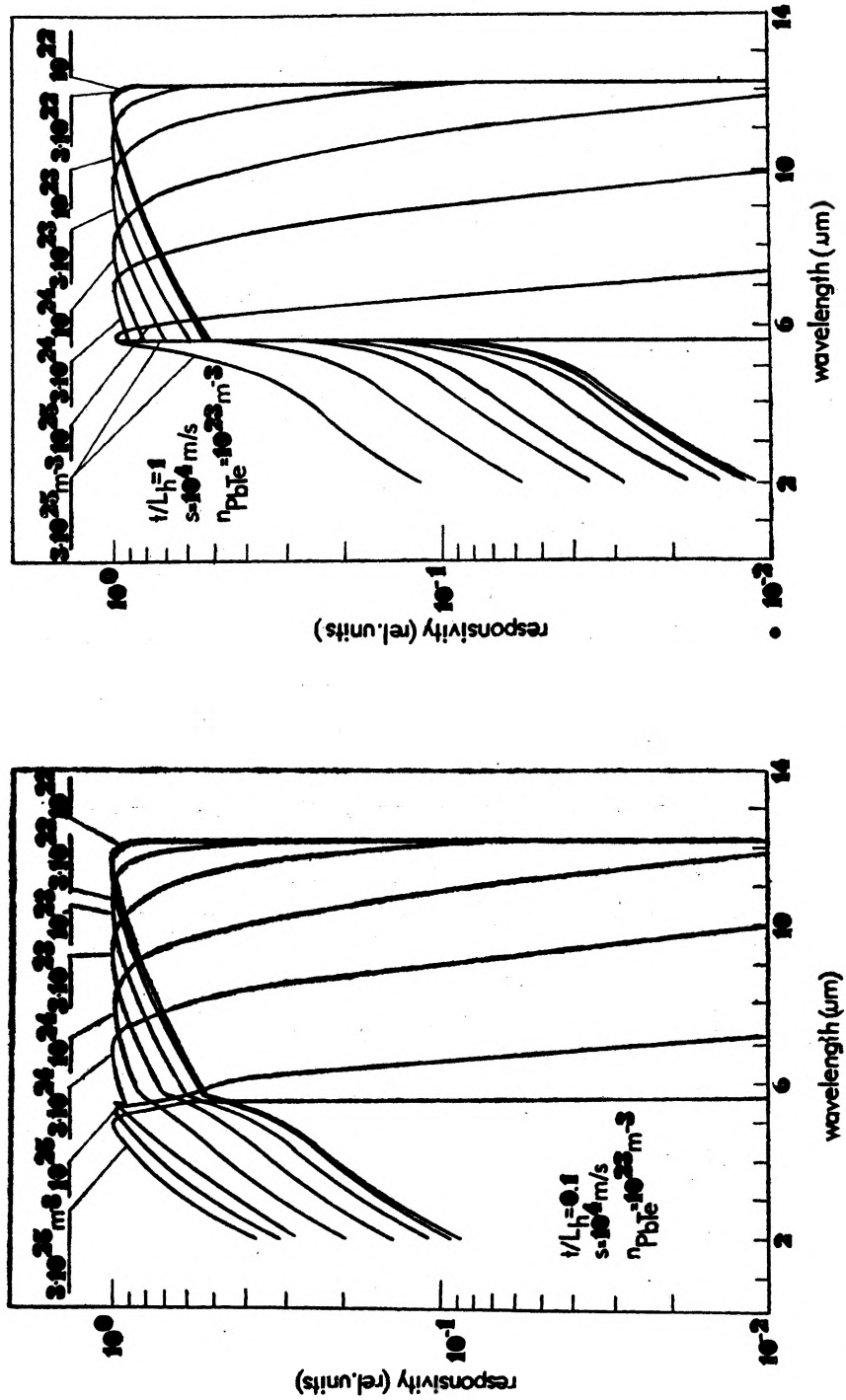

Fig. 3. Calculated spectral responses of sensitivity for *n*-PbTe/*p*-$Pb_{0.78}Sn_{0.22}Te$ heterojunctions at 77 K. Donor concentrations in PbTe–10^{23} m^{-3}, acceptor concentrations $Pb_{0.78}Sn_{0.22}Te$ is marked in figures: a. $t/L_h = 0.1$, $s_1 = 0$; b. $t/L_h = 0.1$, $s_1 = 10^4$ m/s; c. $t/L_h = 1$, $s_1 = 0$; d. $t/L_h = 1$, $s_1 = 10^4$ m/s

from the region of p-type to the region of n-type is slowed down slightly by ΔE_c – see Fig. 1). From the work [13] it follows that no energy discontinuity should be expected in PbTe/$Pb_{0.86}Sn_{0.14}Te$ heterojunctions.

The presence of both the surface states and the defects caused by the misfitting of the lattice and imperfect technological process of heterojunction production is an additional factor complicating the discussion. If the effective life-time of carriers inside or close to the space charge is very short, the electrons and holes generated may recombine quickly instead of being separated by the junction. Consequently, the photocurrent will be diminished. In the case of the considered $Pb_{1-x}Sn_xTe$ ($x \approx 0.20$) heterojunctions the lattice constants are fitted very well (they differ only by 0.3%) while their coefficients of linear expansion are identical. From estimations carried out in the work [13] it follows that the interphase recombination rate in PbTe/$Pb_{0.86}Sn_{0.14}Te$ heterojunctions conditioned by the misfitting of the lattice has no influence on the photocurrent value. Additional defects caused by inappropriate technology used in production of heterojunctions may be a source of other factors increasing the recombination rate and diminishing the photocurrents.

From the above discussion it follows that the formulae (2)–(6) may be employed for calculation of quantum efficiency of heterojunctions of n-PbTe/p-$Pb_{1-x}Sn_xTe$ type.

For calculations of spectral characteristics of sensitivity the following formula was used

$$R_v = \frac{\lambda q}{hc} \eta R,$$

where λ – wavelength, q – electron charge, c – light velocity, R – differential resistance of the diode.

When relative units are used the knowledge of R becomes unnecessary. The parameters required for calculations are collected in Table. The Fermi level and diffusion coefficients are counted in the way described in the Appendix.

The parameters assumed for calculations of spectral sensitivity of n-PbTe/p-$Pb_{0.78}Sn_{0.22}Te$ heterojunctions

	PbTe				$Pb_{0.78}Sn_{0.22}Te$			
	E_F [meV]	D [m²/s]	τ [s]	μ [m²/Vs]	E_F [meV]	D [m²/s]	τ [s]	μ [m²/Vs]
10^{22}	−22	0.016	$3\cdot10^{-7}$	2.5	−15	0.019	$2\cdot10^{-7}$	3
$3\cdot10^{22}$	−14	0.017	10^{-7}	2.5	− 7	0.021	10^{-7}	3
10^{23}	− 6	0.018	$4\cdot10^{-8}$	2.5	3	0.023	10^{-8}	3
$3\cdot10^{23}$	3	0.022	10^{-8}	2.5	14	0.034	10^{-9}	3
10^{24}	16	0.032	10^{-8}	2.5	32	0.044	10^{-10}	2.5
$3\cdot10^{24}$	36	0.054	10^{-9}	2.5	58	0.039	$3\cdot10^{-11}$	1.4
10^{25}	73	0.053	10^{-10}	1.4	102	0.024	10^{-11}	0.55

The life-times given in Table are determined by the interband recombination of Auger and radiative types [20, 21], while the carrier mobility has been accepted after the papers [22, 23].

In Figure 3 the calculated spectral characteristic of *n*-PbTe/*p*-$Pb_{0.78}Sn_{0.22}Te$ in the 77 K temperature are shown. The calculations are carried out for two classical design cases of the photodiode (when $(t+d)\to\infty$, the influence of the recombination rate becomes inessential) illuminated from the PbTe side, i.e. for the optimal construction when $t/L = 0.1$ [24] and when $t/L = 1$. The cases of zero and high (10^4 m/s) surface recombination rates were studied.

It has been assumed that the donor concentration in PbTe is constant and amounts to 10^{23} m^{-3} (for such concentration no influence of the Burstein-Moss effect in this material is observed – see Fig. 1c), whereas the concentration of acceptors in $Pb_{0.78}Sn_{0.22}Te$ is variable, which is marked in Fig. 3. From this figure it may be seen that the Burstein-Moss effect on the spectral characteristics is distinct at the hole concentration above 10^{23} m^{-3} in $Pb_{0.78}Sn_{0.22}Te$. At the concentration above 10^{25} m^{-3} the long wavelength sensitivity limit of heterojunctions is determined by the PbTe region. Such a long shift of λ_c is caused by two effects: the Burstein-Moss effect and the very low lengths of the carrier diffusion path in $Pb_{1-x}Sn_xTe$. Consequently, minimal part of the carriers generated in the region of *p*-type reaches the junction and gives its contribution to the photocurrent. It may be noted that the spectral characteristics of heterojunctions in which the junction is positioned deeply are more selective. The surface recombinations lower the photocurrent in the short wavelength range.

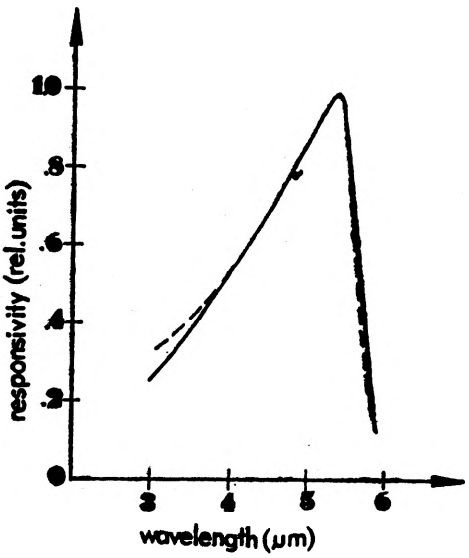

Fig. 4. The relative sensitivity of *C*-1 photodiode at 77 K according to the paper [12] (solid line). The broken line is used to mark the response calculated theoretically and fitted to it for the following parameters: $N_d = 10^{22}\,m^{-3}$, $N_a = 1.5\cdot10^{25}\,m^{-3}$, $x = 0.2$, $x_n/L = 0.04$, $s_1 = 5\cdot10^4$ m/s, $x_n = 2.5$ μm

Also some attempts have been made to fit the theoretically calculated spectral responses of *n*-PbTe/*p*-$Pb_{1-x}Sn_xTe$ heterojunctions. For this purpose we have used some experimental data given in the works from which the measur-

ed spectral responses were taken. The values of the diffusion coefficients and the life-times were evaluated by extrapolating the values given in Table. In Fig. 4 the continuous line is used to show the relative sensitivity of the photodiode C-1 according to [12], while the broken line presents the response calculated theoretically. From the measurements of the C-V characteristics reported in [12] it follows that the concentration of donors in the less dopped region of the junction amounts to about 10^{22} m^{-3}. Therefore, the above electron concentration in PbTe was accepted in calculations. In order to fit correctly the measured characteristics in the short wavelength range it was necessary to assume high value of the surface recombination rate $s_1 = 5 \cdot 10^4$ m/s. The measured characteristics of the B-4 diode at 77 K temperature as reported in [11], as well as the theoretically calculated response best fitted to the previous one, are, in turn, shown in Fig. 5. It should be noted, that the theoretical calculations do not foresee the measured local sensitivity minimum at the 8.5 μm wavelength.

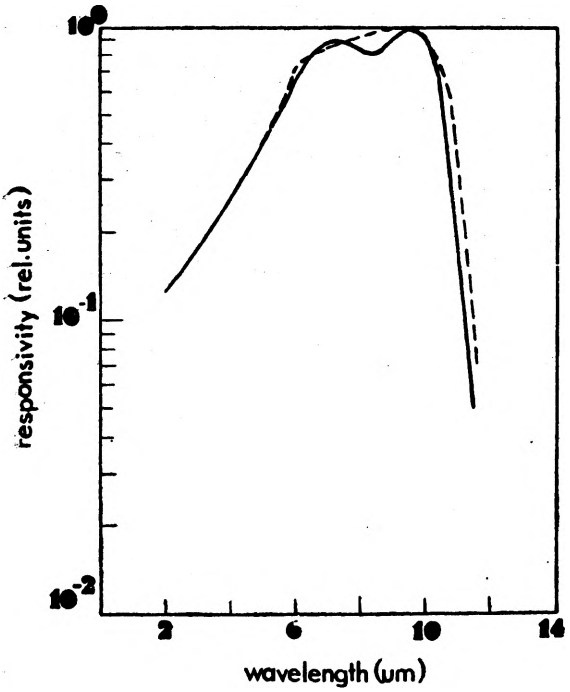

Fig. 5. The relative sensitivity of B-4 photodiode at 77 K according to the paper [11] (continuous line). The broken line is used to mark the response calculated theoretically and fitted to it for the following parameters: $N_d = 10^{22}$ m^{-3}, $N_a = 3 \cdot 10^{23}$ m^{-3}, $x = 0.21$, $x_n/L = 0.05$, $s_1 = 10^4$ m/s, $x_n = 3.2$ μm

Formerly, it was noted that in the case of deeply positioned junctions the spectral characteristics are more selective. The shortwavelength edge is determined by the radiation absorption in the upper energy gap of PbTe, while the spectral cutoff is due to the $Pb_{1-x}Sn_xTe$ material. Such response measured by the authors in [1] is shown in Fig. 6. The n-PbTe/p-$Pb_{1-x}Sn_xTe$ heterojunctions were illuminated from the PbTe monocrystal side of the thickness ~ 250 μm and the electron concentration of about 10^{23} m^{-3}. In order to well fit the longwavelength part of response it should be assumed that the composition of $Pb_{1-x}Sn_xTe$

is 0.22, instead of 0.20 given in [1], and that the concentration in this material is $2 \cdot 10^{23}$ m^{-3}. The surface recombination rate has no influence on the spectral characteristics due to the thick region of PbTe.

The presented results of calculations of spectral responses of the *n*-PbTe/*p* -$Pb_{1-x}S_xTe$ functions confirm the fact that the spectral cutoff limit depends upon

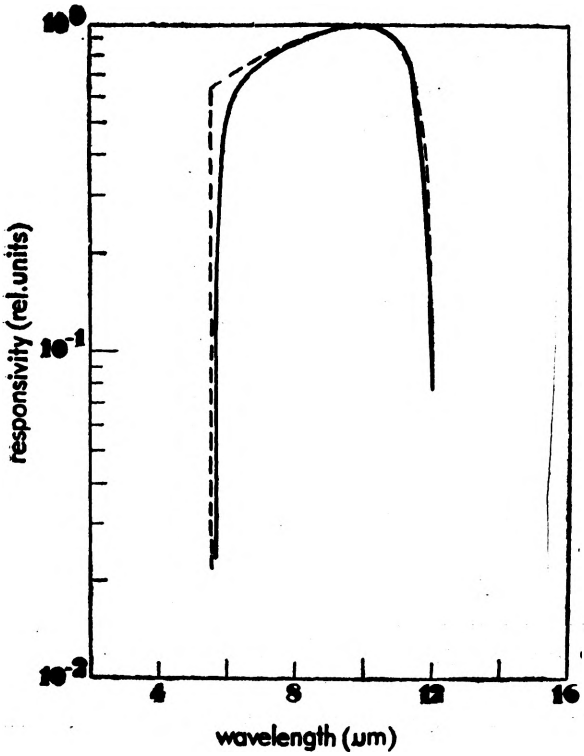

Fig. 6. The relative sensitivity of *n*-PbTe/*p*-$Pb_{1-x}Sn_xTe$ heterojunction according to the paper [1]. The broken line is used to mark the response calculated theoretically and fitted to it for the following parameters: $N_d = 10^{23} \cdot m^{-1}$, $N_a = 2 \cdot 10^{23}$ m^{-3}, $x = 0.22$, $x_n = 250$ μm

the carrier concentration in $Pb_{1-x}Sn_xTe$. The λ_c shift may be influenced also by the diffusion process at the PbTe-$Pb_{1-x}Sn_xTe$ interface [8]. However, for high carrier concentration in $Pb_{1-x}Sn_xTe$ the spectral responses may be determined also by the PbTe semiconductors.

Appendix

Fermi level and effective masses

The calculation of Fermi level has been carried out basing on the Kane model, using the generalized Fermi-Dirac integral. In this method the dependence of the Fermi level E_F upon the carrier concentration is determined by the relation [25]

$$n = \frac{(2m^*_{do}kT)^{1/2}}{3\pi h^2} \int_0^\infty \left(-\frac{\partial f}{\partial z}\right)(z + \beta z)^{3/2} dz, \tag{A1}$$

where $f = \{\exp[(E-E_F)/kT]+1\}^{-1}$ is the Dirac-Fermi distribution function, $z = E/kT$, $\beta = kT/E_g$, E – energy, E_g – energy gap, k – Boltzmann constant, h – Planck constant, m^*_{do} – density-of-state effective mass at the bottom of the band.

On the basis of the work [26] it has been assumed that the effective mass anisotropy coefficient for the longitudinal m_l^* and transverse m_t^* mass components is equal $K = 11$; $m_l^* = 0.146$ m (E_g/eV), $m^*_{do} = N^{2/3}(m_l^* m_t^{*2})^{1/3} = 0.81\ m\ (E_g/\text{eV})$, for $N = 4$, where m denotes the free electron mass.

Coefficient of diffusion

In the state of thermal equilibrium the thermal coefficient of carrier diffusion in the semiconductor of n-type is [27]

$$D_e = -\frac{\mu_e}{q}\frac{\int_0^\infty g(E)f_c(E)\,dE}{\int_0^\infty g(E)\frac{\partial f_c}{\partial E}\,dE}, \tag{A2}$$

where μ_e – electron mobility.

By substituting both the state density function according to the Kane model [25]

$$g(E) = \frac{(2m^*_{do})^{3/2}}{4\pi^2\hbar^3}\left[E\left(1+\frac{E}{E_g}\right)\right]^{1/2}\left(1+\frac{2E}{E_g}\right), \tag{A3}$$

and the Fermi function f_c and assuming that $\eta = E_F/kT$ we obtain

$$D_e = \frac{\frac{\mu_e}{q}kT\int_0^\infty [z(1+2\beta z)]^{1/2}(1+2\beta z)(e^{z-\eta}+1)^{-1}dz}{\int_0^\infty [z(1+2\beta z]^{1/2}(1+2\beta z)e^{z-\eta}(e^{z-\eta}+1)^{-2}dz}. \tag{A4}$$

In the case of nondegenerated semiconductors this expression may be reduced to the Einstein formula

$$D_e = \frac{kT}{q}\mu_e.$$

Due to the symmetry of the band structure of lead and tin chalkogenides $D_e \approx D_h$.

References

[1] ANDREWS A.M., LONGO J.T., CLARKE J.E., GERTNER E.R., Appl. Phys. Lett. **26** (1975), 438.

[2] WANG C.C., KALISHER M.H., TRACY J.M., CLARKE J.E., LONGO J.T., Solid-State Electron. **21** (1978), 625.

[3] WANG C.C., KIM M.E., J. Appl. Phys. **50** (1979), 3733.

[4] CHIA P.S., BALON J.R., LOCKWOOD A.H., RANDALL D.M., RENDA F.J., DE VAUX L.H., KIMURA H., Infrared Phys. **15** (1975), 279.

[5] WANG C.C., HAMPTON S.R., Solid-State Electron **18** (1975), 121.

[6] KOSOGOV O.V., KIM GVAP DE, MARAMZINA M.A., GIRICH B.G., NIKOLAEV M.I., PELEVIN O.V., TEREHOVICH T.F., Fiz. Tekh. Poluprov. **11** (1977), 1902.

[7] Stafeev V.I., Banin E.S., Gusarov A.V., Terehovich T.F., Pelevin O.V., Nikolaev M.I., Fiz. Tekh. Poluprov. **12** (1978), 1714.
[8] Stafeev V.I., Banin E.S., Terehovich T.F., Mironova O.A., Pelevin O.V., Girich B.I., Mohovaya T.G., Nikolaev M.I., Fiz.Tekh.Poluprov. **12** (1978), 1723.
[9] Kasai I., Basset D.W., Hornung J., J.Appl.Phys. **47** (1976), 3167.
[10] Igras E., Rogalski A., Electron Technol. **10** (1977), 471.
[11] Rogalski A., Electron Technology, to be published.
[12] Rogalski A., Thin Solid Films **67** (1980), 179.
[13] Bittner H., Bremser W., Herrmann K.H., *Proc. 9th Symp. of the IMEKO Technical Committee on Photon Detectors*, Budapest 1980.
[14] Genzow D., Herrmann K.H., Kostial H., Rechenberg J., Yunovich E.E., Phys. Stat. Sol. (b) **86** (1978), K21.
[15] Genzow D,, Mironow A.G., Ziep O., Phys. Stat. Sol. (b) **90** (1978), 535.
[16] Zemel J.N., Jensen J.D., Schoolar R.B., Phys. Rev **140** (1965), A330.,
[17] Lowney J.R., Senturia S.D., J. Appl. Phys. **47** (1976), 1771.
[18] Hovel H.J., *Semiconductors and Semimentals* (edited by R.K. Willardson and A.C. Beer), Vol. 11, Academic Press, New York, San Francisco, London 1975.
[19] Milnes A.G., Feucht D. L., *Heterojunctions and Metal-Semiconductor Junctions*, Academic Press, New York and London 1972.
[20] Ziep O., Genzow D., Mocker M., Herrmann K.H., Phys. Stat. Sol. (b) **99**, (1980), 129.
[21] Grudzień M., Rogalski A., Infrared Phys. **21** (1981), 1.
[22] Ravich Yu. I., Efimova A.B., Tamarchenko V.I., Phys. Stat. Sol. (b) **45** (1973), 453.
[23] Sizov F.F., Lashkareev G. V., Radchenko M.V., Orletskii V.B., Grigorovich E.T., Fiz. Tekh. Poluprov. **10** (1976), 1801.
[24] Rogalski A., Rutkowski J., Infrared Physics, to be published.
[25] Kołodziejczak J., Acta Phys. Pol. **20** (1961), 289.
[26] Gureev D.M., Zasavitski I.I., Natsonashvili B.N., Shotow A.P., Fiz.Tekh. Poluprov. **12** (1978), 708.
[27] Smith R.A., *Półprzewodniki*, PWN, Warszawa 1966 (in Polish).

Received August 18, 1981

Спектральные характеристики гетероструктур *n*-PbTe/*p*-$Pb_{1-x}Sn_x$ Te

Проанализировано влияние эффекта Бурштейна-Мосса на спектральную зависимость коэффициента поглощения $Pb_{1-x}Sn_xTe$ и на спектральные характеристики гетероструктур *n*-PbTe/*p*-$Pb_{1-x}Sn_xTe$. Доказано, что при концентрации носителей в $Pb_{1-x}Sn_xTe$ выше 10^{25} м$^{-3}$ длинноволновой предел чувствительности гетероструктур определён материалом PbTe. Предприяты также попытки согласования теоретически рассчитанных характеристик этого типа гетероструктур с экспериментально измеренными.